[Communication] www.whxb.pku.edu.cn

单根(7,5)蛇形单壁碳纳米管的拉曼光谱

谢黎明 于学春 冯超群 张 锦* 刘忠范
(北京大学化学与分子工程学院, 分子动态与稳态结构国家重点实验室, 北京分子科学国家实验室, 北京 100871)

摘要: 研究了单根(7,5)蛇形单壁碳纳米管的拉曼光谱特征, 观察到了环呼吸振动峰(RBM)、环呼吸振动的倍频峰(2RBM)、介于中间频率的振动峰(IMF)、无规振动峰(*D*)、剪切振动峰(*G*)、中间频率振动峰(*M*)、剪切振动和环呼吸振动的和频峰(*G*+RBM)、面内横向光学声子和纵向声学声子的和频峰(iTOLA)、无规振动的二次共振峰(*G*′或者 2*D*)以及其它一些归属不清楚的拉曼峰. 不同激发波长和不同激发偏振拉曼光谱研究表明, 这些拉曼光谱峰显示出了非常强的激发能量和激发偏振的选择性.

关键词: 拉曼光谱; (7,5)单壁碳纳米管; 共振拉曼光谱; 偏振拉曼光谱
中图分类号: O649

Raman Characterization of a Highly Folded Individual Serpentine (7,5) Single-Walled Carbon Nanotube

XIE Li-Ming YU Xue-Chun FENG Chao-Qun ZHANG Jin* LIU Zhong-Fan
(*Beijing National Laboratory for Molecular Sciences, State Key Laboratory for Structural Chemistry of Unstable and Stable Species, College of Chemistry and Molecular Engineering, Peking University, Beijing 100871, P. R. China*)

Abstract: We carried out Raman characterization of a highly folded individual serpentine (7,5) single-walled carbon nanotube (SWNT). Twenty five Raman peaks were observed, which included a radial breathing mode (RBM band), an overtone of RBM (2RBM band), an immediate-frequency band (IMF band), a disorder-induced band (*D* band), a tangential band (*G* band), an *M* band (1700–1900 cm^{-1}), a combination mode of *G* and RBM (*G*+RBM band), a combination mode of in-plane transverse optic (iTO) phonon and longitudinal acoustic (LA) phonon (iTOLA band), an overtone of the *D* band (*G*′ or 2*D* band), an overtone of the *G* band (2*G* band) and some other bands with unknown assignments. Further Raman measurements at different laser excitation wavelengths and different excitation polarization show that these Raman peaks are highly dependent on the excitation energy and the excitation polarization.

Key Words: Raman spectroscopy; (7,5) Single-walled carbon nanotube; Resonance Raman spectroscopy; Polarization Raman spectroscopy

Raman spectroscopy is a powerful approach to characterize structure, electronic properties, and phonon properties of SWNTs[1–4]. When SWNTs are resonant with the incident laser, where the incident laser energy is close to the excitonic transition energies (E_{ii}) of SWNTs, the Raman intensity of SWNTs can be enhanced by 10^3 times[3]. Usually observed resonant Raman bands of SWNTs are RBM band (100–400 cm^{-1}), *D* band (ca 1350 cm^{-1}), *G* band (ca 1580 cm^{-1}), and *G*′ band (ca 2700 cm^{-1})[1]. The frequency of RBM is inverse to the diameter of SWNTs, which is widely used to assign (*n*,*m*) indices of SWNTs[4–6]. The RBM and *G* bands are first-order Raman peaks, while the *D* and *G*′ bands are intervalley second-order Raman peaks[2].

Received: October 13, 2009; Revised: December 8, 2009; Published on Web: February 9, 2010.
*Corresponding author. Email: jinzhang@pku.edu.cn; Tel: +86-10-62752555.
The project was supported by the National Natural Science Foundation of China (20673004, 20725307, 50821061) and National Key Basic Research Program of China (973) (2006CB932701, 2006CB932403, 2007CB936203).
国家自然科学基金(20673004, 20725307, 50821061)和国家重点基础研究发展计划项目(973) (2006CB932701, 2006CB932403, 2007CB936203)资助

There are also other weak second-order Raman bands observed in SWNTs, such as 2RBM band[7–8], IMF band (700–900 cm^{-1})[9–11], *M* band (1700–1800 cm^{-1})[12–13], *G*+RBM band (1700–2000 cm^{-1})[14], iTOLA band (1700–2000 cm^{-1})[13], and 2*G* band (ca 3200 cm^{-1})[15]. These weak second-order Raman bands can give rich fundamental information of SWNTs. For example, the overtone of RBM has been used to determine electron-phonon coupling in SWNTs[7–8].

However, for an individual SWNT, it is hard to observe all of these weak Raman bands even at strong resonance. SWNT bundles and SWNT solutions may give stronger Raman intensity than an individual SWNT, but Raman bands from different (*n*,*m*) SWNTs in bundles or in solution are overlapped, which makes it difficult to investigate structure-dependent electronic and phonon properties of SWNTs.

Serpentine SWNTs, which have high-density parallel SWNT sections[16–17], can give much stronger Raman intensity than an individual section. Additionally, serpentine SWNT sections are not bundled with each other. Therefore, serpentine SWNTs can be used to observe various second-order Raman bands from individual SWNTs without nanotube–nanotube interactions. Here, we have grown a highly folded (20 sections/μm) individual serpentine SWNT. Raman characterization was carried out on this highly folded individual serpentine SWNT and 25 Raman peaks have been observed, including RBM band, *D* band, *G* band, *G*′ band, various second-order Raman bands, and some bands with unclear assignments (labeled as NC1 to NC3).

1 Experimental

Serpentine SWNTs were grown on quartz by following the method in references[16–17]. Atomic force microscope (AFM) characterization was conducted on DI NANOSCOPE III (Veeco Instruments, USA). Scanning electron microscope (SEM) characterization was conducted on Hitachi S-4800 (Japan). Raman characterization was conducted on a Horiba HR800 Raman system. A 100× objective was used to focus laser beam and to collect Raman signal.

2 Results and discussion

Figs.1(a) and 1(b) show a scanning electron microscope (SEM) image and an atomic force microscope (AFM) image of the same individual serpentine SWNT. The distance between two nearest folded sections of this serpentine SWNT is about 50 nm. From section analysis in the AFM image (the inset in Fig.1(b)), the diameter is measured to be (0.8±0.1) nm for this SWNT , which indicates an individual SWNT.

Fig.1(c) shows a Raman spectrum of this SWNT excitated at 633 nm. The polarization direction of the excitation laser is parallel to the axial direction of the SWNT sections. Apart from Raman peaks from the quartz substrate (labeled as ＊), a bunch of Raman peaks were observed from this individual SWNT. The strong peak at 290 cm^{-1} is assigned to RBM band. The reported RBM frequencies for (7,5) and (8,3) are 283 and 297 cm^{-1} [6], respectively. The second excitonic transition energies (E_{22}) for (7,5) and (8,3) are 647 and 663 nm[6], respectively. Additionally, E_{ii} of SWNTs shifts slightly with dielectric surroundings (< 30 meV, i.e., about 10 nm around 650 nm)[18]. Therefore, this SWNT is assigned to (7,5) because the RBM intensity is extremely strong and the E_{22} of (7,5) nanotube is more close to excitation energy (633 nm). The diameter measured with AFM ((0.8±0.1) nm) is consistent with the calculated diameter for a (7,5) nanotube (0.82 nm). All the Raman bands in Fig.1(c) are zoomed in Fig.2, where overlapped peaks are fitted by multi-lorentzian functions.

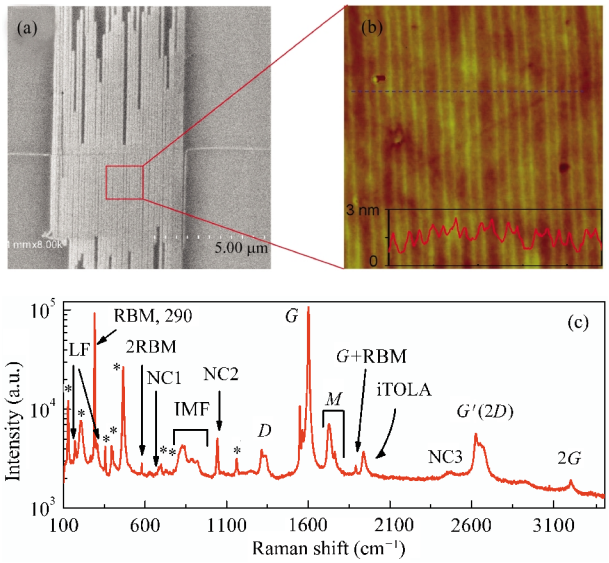

Fig.1 SEM and AFM images and Raman spectrum of a serpentine SWNT

(a) SEM image of a serpentine SWNT, (b) AFM image of the serpentine SWNT in (a) and the image size is 1 μm×1 μm, the inset in (b) is the section analysis along the blue dash line in (b); (c) Raman spectrum of the serpentine SWNT at 633 nm excitation with laser polarization parallel to SWNT. The Raman peaks labeled as ＊ were from the substrate (quartz). LF: low-frequency band; NC1, NC2, and NC3: Raman bands with unclear assignment

In Fig.2(a), the 290 cm^{-1} peak is the RBM. The 580 cm^{-1} peak is assigned to 2RBM. The assignment for three low frequency (LF) bands at 169, 174, and 306 cm^{-1} is unclear. They may be double resonance of transverse acoustic (TA) phonon and/or longitudinal acoustic (LA) phonon which has been observed in graphite whisker[19]. In Fig.2(b), 824, 841, 885, and 919 cm^{-1} peaks are assigned to IMF band. The IMF band is the combination modes of out-of-plane transverse optic (oTO) phonon and LA phonon[9–11]. The assignment for the peaks at 682 and 1042 cm^{-1} is unknown. Dresselhaus *et al.*[11] assigned that peak around 1042 cm^{-1} to Raman peak of C-O-C. In Fig.2(c), the 1315 and 1337 cm^{-1} peaks are assigned to *D* band. The 1549, 1563, 1583, and 1601 cm^{-1} peaks are assigned to *G* band. The 1728 and 1763 cm^{-1} peaks are assigned to *M* band, which is the overtone of the oTO phonon (oTO phonon frequency is at 867 cm^{-1} in graphite)[13]. The two *M* bands (M^- at 1728 cm^{-1} and M^+ at 1763 cm^{-1}) are corresponding to different resonance processes[13]. The 1891 cm^{-1} peak is assigned to *G*+RBM band according to its frequency. The 1940 cm^{-1} peak is assigned to iTOLA band. In Fig.2(d), the 2662 and

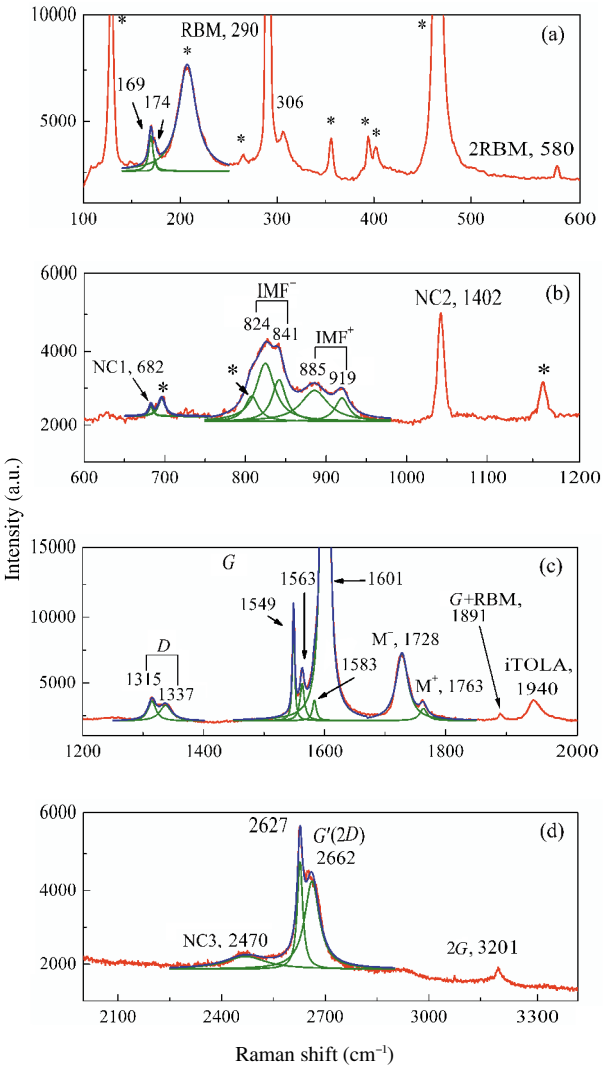

Fig.2 Zoomed Raman spectra of the serpentine SWNT in Fig.1

range: (a) 100–600 cm^{-1}, (b) 600–1200 cm^{-1}, (c) 1200–2000 cm^{-1}, (d) 2000–3400 cm^{-1}; The blue lines are multi-lorentzian fitting results and the green lines are fitted individual peaks.

2627 cm^{-1} peaks are assigned to intervalley double resonance of *K*-point phonon (*G′* band). The 3201 cm^{-1} peak is assigned to overtone of 1601 cm^{-1} *G* band. The assignment for the 2470 cm^{-1} peak is not clear. It may be inter-electronic band double resonance of *K*-point phonon.

Further, Raman measurement was carried out at 514 nm excitation with laser polarization parallel to SWNT (Fig.3(a)) and at 633 nm excitation with laser polarization perpendicular to SWNT (Fig.3(b)). Compared with Raman spectrum at 633 nm excitation with parallel configuration (Fig.3(c)), only weak *G* band, whose intensity decreased by ca 200 times, was observed at 514 nm excitation. This suggests that all Raman peaks observed in Fig.1(c) and Fig.2 are resonance Raman peaks. Excitation at 633 nm with laser polarization perpendicular to SWNT only gives very week RBM and *G* band (Fig.3(b)), which is consistent with perfectly parallel-aligned SWNT sections (Fig.1(b)).

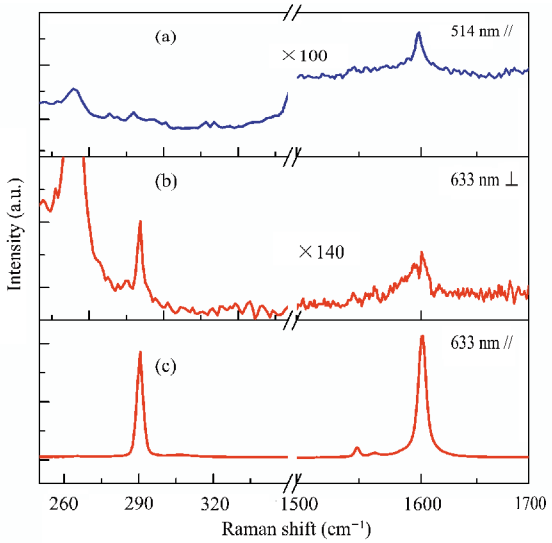

Fig.3 Raman spectra of the serpentine SWNT at different wavelengths and different excitation polarization

(a) at 514 nm excitation with laser polarization parallel to SWNT, (b) at 633 nm excitation with laser polarization perpendicular to SWNT, (c) at 633 nm excitation with laser polarization parallel to SWNT

3 Conclusions

In conclusion, we have observed RBM, LF, 2RBM, IMF, *D*, *G*, *M*, *G*+RBM, *G′*, 2*G* bands and some other bands from a highly folded individual serpentine (7,5) SWNT at 633 nm parallel excitation. Since 2RBM[7-8], IMF[10] bands, and possibly LF, *M*, and *G*+RBM bands, are charity-dependent, these weak second-order Raman bands may be useful for (*n*,*m*) assignment.

Acknowledgments: We thank Prof. Mildred Dresselhaus (Massachusetts Institute of Technology, USA), Prof. Jing Kong (Massachusetts Institute of Technology, USA), and Prof. Riichiro Saito (Tohoku University, Japan) for their useful discussion.

References

1 Dresselhaus, M. S.; Dresselhaus, G.; Jorio, A.; Souza, A. G.; Pimenta, M. A.; Saito, R. *Acc. Chem. Res.*, **2002, 35**: 1070

2 Dresselhaus, M. S.; Dresselhaus, G.; Saito, R.; Jorio, A. *Physics Reports-Review Section of Physics Letters*, **2005, 409**: 47

3 Rao, A. M.; Richter, E.; Bandow, S.; Chase, B.; Eklund, P. C.; Williams, K. A.; Fang, S.; Subbaswamy, K. R.; Menon, M.; Thess, A.; Smalley, R. E.; Dresselhaus, G.; Dresselhaus, M. S. *Science*, **1997, 275**: 187

4 Maultzsch, J.; Telg, H.; Reich, S.; Thomsen, C. *Phys. Rev. B*, **2005, 72**: 205438

5 Meyer, J. C.; Paillet, M.; Michel, T.; Moreac, A.; Neumann, A.; Duesberg, G. S.; Roth, S.; Sauvajol, J. L. *Phys. Rev. Lett.*, **2005, 95**: 217401

6 Bachilo, S. M.; Strano, M. S.; Kittrell, C.; Hauge, R. H.; Smalley, R. E.; Weisman, R. B. *Science*, **2002, 298**: 2361

7 Yin, Y.; Vamivakas, A. N.; Walsh, A. G.; Cronin, S. B.; Unlu, M.

S.; Goldberg, B. B.; Swan, A. K. *Phys. Rev. Lett.*, **2007, 98**: 037404

8 Shreve, A. P.; Haroz, E. H.; Bachilo, S. M.; Weisman, R. B.; Tretiak, S.; Kilina, S.; Doorn, S. K. *Phys. Rev. Lett.*, **2007, 98**: 037405

9 Fantini, C.; Jorio, A.; Souza, M.; Ladeira, L. O.; Souza, A. G.; Saito, R.; Samsonidze, G. G.; Dresselhaus, G.; Dresselhaus, M. S.; Pimenta, M. A. *Phys. Rev. Lett.*, **2004, 93**: 087401

10 Luo, Z. T.; Papadimitrakopoulos, F.; Doorn, S. K. *Phys. Rev. B*, **2007, 75**: 205438

11 Fantini, C.; Jorio, A.; Souza, M.; Saito, R.; Samsonidze, G. G.; Dresselhaus, M. S.; Pimenta, M. A. *Phys. Rev. B*, **2005, 72**: 085446

12 Zhao, J. L.; Jiang, C. Y.; Fan, Y. W.; Burghard, M.; Basche, T.; Mews, A. *Nano Lett.*, **2002, 2**: 823

13 Brar, V. W.; Samsonidze, G. G.; Dresselhaus, M. S.; Dresselhaus, G.; Saito, R.; Swan, A. K.; Unlu, M. S.; Goldberg, B. B.; Souza, A. G.; Jorio, A. *Phys. Rev. B*, **2002, 66**: 155418

14 Brown, S. D. M.; Corio, P.; Marucci, A.; Pimenta, M. A.; Dresselhaus, M. S.; Dresselhaus, G. *Phys. Rev. B*, **2000, 61**: 7734

15 Wang, F.; Liu, W. T.; Wu, Y.; Sfeir, M. Y.; Huang, L. M.; Hone, J.; O′Brien, S.; Brus, L. E.; Heinz, T. F.; Shen, Y. R. *Phys. Rev. Lett.*, **2007, 98**: 047402

16 Geblinger, N.; Ismach, A.; Joselevich, E. *Nat. Nanotechnol.*, **2008, 3**: 195

17 Yao, Y.; Dai, X.; Feng, C.; Zhang, J.; Liang, X.; Ding, L.; Choi, W.; Choi, J.; Kim, J. M.; Liu, Z. *Adv. Mater.*, **2009, 21**: 4158

18 Ohno, Y.; Iwasaki, S.; Murakami, Y.; Kishimoto, S.; Maruyama, S.; Mizutani, T. *Phys. Rev. B*, **2006, 73**: 235427

19 Tan, P. H.; Hu, C. Y.; Dong, J.; Shen, W. C.; Zhang, B. F. *Phys. Rev. B*, **2001, 6421**: 214301